ISSN (Print) 1226-1750
ISSN (Online) 2233-6656
Journal of Magnetics 21(1), 51-56 (2016) http://dx.doi.org/10.4283/JMAG.2016.21.1.051

Effect of Grain Boundary Modification on the Microstructure and Magnetic Properties of HDDR–treated Nd–Fe–B Powders

Shu Liu[1,2], Nam-Hyun Kang[2], Ji-Hun Yu[1], Hae-Woong Kwon[3], and Jung-Goo Lee[1]*

[1]Powder & Ceramics Division, Korea Institute of Materials Science, 797 Changwondaero, Changwon 51508, Korea
[2]Department of Materials Science and Engineering, Pusan National University, Busandaehak-ro 63 beon-gil, Geumjeong-gu, Busan 46241, Korea
[3]Department of Materials Science and Engineering, Pukyong National University, Yongso-ro 45 Nam-gu, Busan 48513, Korea

(Received 31 December 2015, Received in final form 11 March 2016, Accepted 13 March 2016)

The microstructure and magnetic properties of HDDR–treated powders after grain boundary diffusion process (GBDP) with Nd–Cu alloy at different temperatures have been studied. The variation of GBDP temperature had multifaceted influences on the HDDR–treated powders involving the microstructure, phase composition and magnetic performance. An enhanced coercivity of 16.9 kOe was obtained after GBDP at 700 °C, due to the modified grain boundary with fine and continuous Nd–rich phase. However, GBDP at lower or higher temperature resulted in poor magnetic properties because of insufficient microstructural modification. Especially, the residual hydrogen induced phenomenon during GBDP strongly depended on the GBDP temperature.

Keywords : Nd–Fe–B magnets, HDDR, Nd–Cu alloy, residual hydrogen

1. Introduction

The Nd–Fe–B permanent magnets have been widely used as indispensable materials for various kinds of motors and actuators due to their excellent magnetic properties and cost performances [1]. Especially, high efficiency traction motors for hybrid electric vehicles (HEVs) or electric vehicles (EVs) is one of the most rapidly growing areas [2]. For these applications, higher coercivity than that required for other applications is needed to withstand the demagnetization problem at the high operation temperature of the motor (~200 °C). The temperature coefficient of coercivity has a largely negative value; it means the coercivity decreases rapidly as the temperature increases, which is the main drawback of Nd–Fe–B magnets. In order to overcome this problem, one of the most effective solutions is doping heavy rare earth (HRE) element such as Dy or Tb into the Nd–Fe–B magnets, which cause the large coercivity enhancement at room temperature. However, the enhancement of coercivity by the doping of HRE elements can only be achieved at the expense of the maximum energy product, due to the reduction in the magnetization via the antiferromagnetic coupling between the magnetic moments of HRE elements and Fe element [3]. Moreover, the natural abundance of HRE elements is quite low and their material prices are unstable. Thus, achieving high coercivity without HRE elements is an urgent issue for high–temperature motor application of Nd–Fe–B permanent magnets. Intensive studies have been focused on producing high coercivity Nd–Fe–B magnets without HRE elements [4-6] and it is now well known that the coercivity is strongly influenced by the microstructures such as grain size and grain boundary (GB) [7-9]. With regard to the former, the coercivity increases with the decrease of grain size down to the single domain size (~250 nm). The hydrogenation–disproportionation–desorption–recombination (HDDR) process is one of the most effective methods to produce anisotropic Nd–Fe–B magnetic powders with single domain–sized grains [10]. However, the reported highest coercivity of HDDR–treated Nd–Fe–B powders without HRE was disappointingly low considering from the ultrafine grain size [11]. The poor coercivity of HDDR–treated Nd–Fe–B powders with nearly single domain–sized

*Corresponding author: Tel: +82-55-280-3606
Fax: +82-55-280-3289, e-mail: jglee36@kims.re.kr

grains is attributed to the insufficient control of the Nd–rich GB phase which is significantly important to induce magnetic decoupling between grains [12]. The magnetic decoupling is essential to enhance the coercivity of fine grained magnets [13]. Many studies have demonstrated that the addition of some alloy additives or trace elements, such as Pr, Cu, Nd, Al, and Ga, can efficiently improve the coercivity [13-15]. In other words, the homogenous distribution of Nd–rich phase through the GBs among $Nd_2Fe_{14}B$ main phases can significantly increase the coercivity of fine–grained Nd–Fe–B magnets [16]. On the other hand, it is recently reported that HDDR–treated Nd–Fe–B powders contain a significant amount of the residual hydrogen [17]. Matin et al. have found the coercivity of HDDR–treated Nd–Fe–B powders was significantly reduced after heat treatment due to the residual hydrogen [18]. However, there is no report on the effect of the residual hydrogen during grain boundary diffusion process (GBDP).

In the present work, GB phase of HDDR–treated Nd–Fe–B magnetic powders was modified by GBDP with Nd–Cu alloy. The effect of GBDP with Nd–Cu alloy on the microstructure and magnetic properties of HDDR–treated Nd–Fe–B powders has been studied. Furthermore, the temperature effect of GB modification with Nd–Cu alloy on the phases and microstructures has been discussed.

2. Experimental

The starting powders with a normal composition of $Fe_{80.4}Nd_{12.5}B_{5.7}Nb_{0.4}Ga_{0.8}Co_{0.2}$ (at.%) were produced by the standard HDDR process [19]. The average particle size and grain size of the powders was 100 μm and 300 nm, respectively. The $Nd_{70}Cu_{30}$ (at.%) alloy were arc melted to ingot and then melt-spun to ribbons, followed by vacuum ball milling to particle size of smaller than 4.5 μm. The $Nd_{70}Cu_{30}$ (at.%) powders mixed with the HDDR–treated powders at mass fractions of 6%. The mixed powders were then subjected to GBDP in vacuum at 600, 700 and 800 °C for 3 h, respectively. After that, the powders were quickly gas–quenched to room temperature (RT). The magnetic properties of the powders were measured by a vibrating sample magnetometer (VSM) at RT. For the VSM measurement, the powders mixed with paraffin were aligned and magnetized under 1.5 T static magnetic field and 5 T pulsing magnetic field, respectively. The microstructure and morphology of the powders were analyzed by powder X-ray diffraction (XRD), scanning electron microscopy (SEM) and transmission electron microscopy (TEM).

3. Results and Discussion

Figure 1 shows the SEM images of the initial HDDR–treated powders (a, b), and the powders after GBDP with 6 wt.% Nd–Cu alloy at 600 °C (c, d), 700 °C (e, f) and 800 °C (g, h) for 3 h, respectively. The SEM images of the fractured surface show that the grain size of the initial HDDR–treated powders is around 300 ± 50 nm (Fig. 1(a)) and no significant change in the grain size was observed after GBDP at 600 °C (Fig. 1(c)) and 700 °C (Fig. 1(e)). It should be noted that $Nd_2Fe_{14}B$ grains are surrounded by thin GB layers (arrowed) after GBDP treatment at 700 °C as shown in Fig. 1(e). Further increase of the GBDP temperature up to 800 °C, resulted in the grain growth up to 450 ± 50 nm. In the backscattered electrons (BSE) images, dark and bright contrast region corresponds to

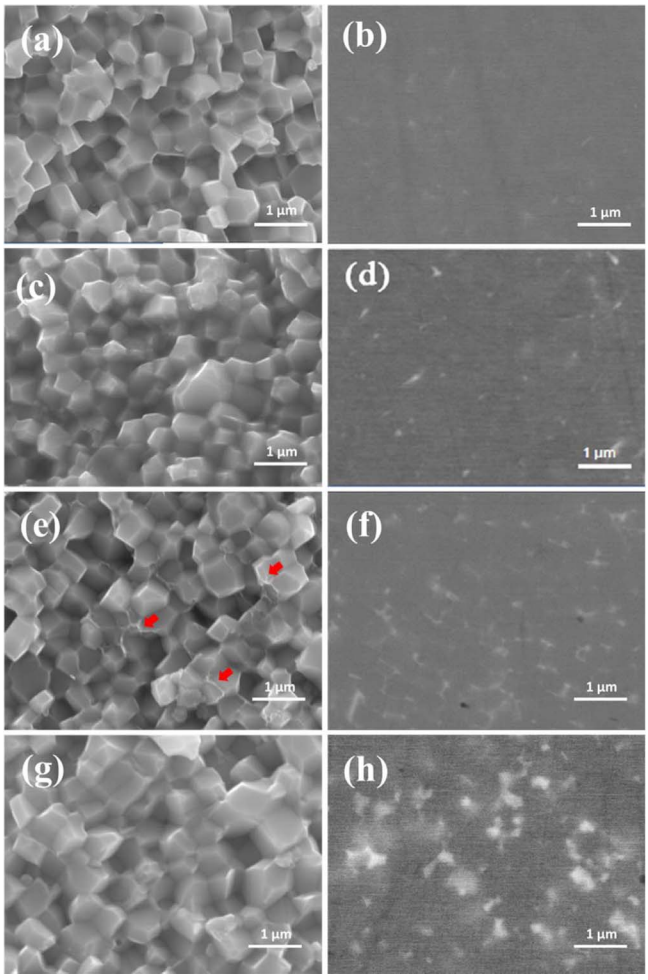

Fig. 1. (Color online) SEM images of the initial HDDR–treated powders, and the powders after GBDP with 6 wt.% Nd–Cu alloy at 600, 700 and 800 °C for 3 hours, respectively. (a), (c), (e), (g) : SE mode image of the fractured surface, and (b), (d), (f), (h) : BSE mode image of the cross–section surface.

$Nd_2Fe_{14}B$ main phase and Nd–rich GB phase, respectively. All samples consist of two contrast regions. However the relative fraction and distribution of the bright contrast area are different among the samples. It is quite difficult to find Nd–rich GB phase in the initial HDDR–treated powder (Fig. 1(b)). The bright region slightly increase but its distribution is not uniform after GBDP at 600 °C (Fig. 1(d)), which indicates that there is no significant enrichment of Nd–rich phase along the GBs. For the powders after GBDP at 700 °C, the bright regions are much more uniformly distributed along the GBs as shown in Fig. 1(f), revealing that the Nd–rich phase is fine and uniformly distributed not only at the triple junction but also along the GBs. These microstructural features suggest that low melting point binary Nd–Cu alloy melted and infiltrated into the HDDR–treated powders, and further induced the formation of Nd–rich phase through the GBs during heat treatment. With further increase of GBDP temperature up to 800 °C, the Nd–rich phase aggregated to the triple junctions and became indistinguishable again along the GBs (Fig. 1(h)). The absence of Nd–rich phase at the GBs can lead to the magnetic coupling among the $Nd_2Fe_{14}B$ main phases [20].

Figure 2 shows the XRD patterns of the initial HDDR–treated powders and the powders after GBDP with 6 wt.% Nd–Cu alloy at 600, 700 and 800 °C for 3 h, respectively. It can be clearly observed that the main characteristic peaks for all these samples correspond to the $Nd_2Fe_{14}B$ phase. It is interested to note that the diffraction peaks after GBDP at 600 and 800 °C were shifted toward higher angles compared with those of the initial HDDR–treated powder (Fig. 2(b)), which indicates that the lattice of the tetragonal $Nd_2Fe_{14}B$–type phase was shrunk after GBDP. Quite recently, it was reported that the HDDR–treated Nd–Fe–B–type magnetic powders contained a significant amount of hydrogen in the form of $Nd_2Fe_{14}BH_x$ hydride, which would be disproportionate into α–Fe, Fe_2B and NdH_2 phase during heat treatment above a threshold temperature [18]. So the lattice shrinkage in Fig. 2 can be attributed to the release of residual hydrogen from the HDDR–treated powders during GBDP. In addition, the peaks for the disproportionated phases of α–Fe, Fe_2B could be clearly confirmed after GBDP at 600 and 800 °C, which indicates that degassing and disproportionation is a dominant phenomenon in the HDDR–treated powders during heat treatment at 600 and 800 °C. This result is consistent with the fact that the threshold temperature for disproportionation is around 600 °C [21]. On the other hand, there is no shift of the diffraction peaks after GBDP at 700 °C compared with those of the initial HDDR–treated powder, and the Fe_2B was not detected.

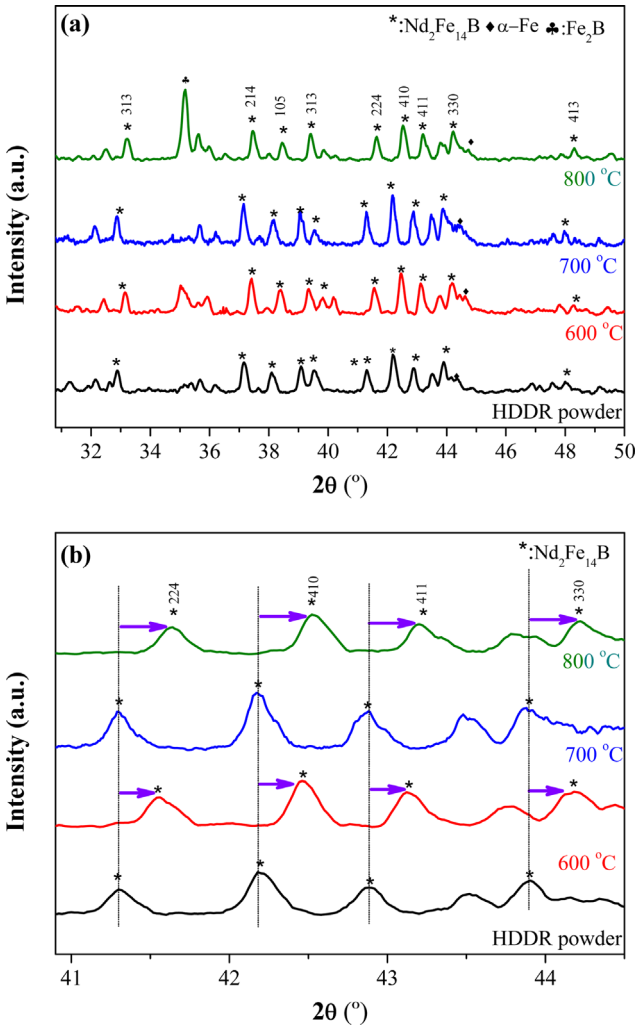

Fig. 2. (Color online) XRD patterns of the initial HDDR–treated powders and the powders after GBDP with 6 wt.% Nd–Cu alloy at 600, 700 and 800 °C for 3 hours, respectively (b) enlarged view of angle shift.

More detailed microstructural observation was carried out using TEM. Figure 3 shows energy–filtered elemental mapping images and high–magnification bright field images of the powders after GBDP with Nd–Cu alloy at 800 °C. It can be confirmed that the α–Fe and Fe_2B phases were formed in the HDDR–treated powders after GBDP at 800 °C (Fig. 3(c) and (f)). This result is consistent with XRD result in Fig. 2.

From these results, it seems that the molten and diffused Nd–Cu alloy along GBs play a role in not only isolating the main phase but also preventing degassing of hydrogen from the HDDR–treated powders. However, further studies are needed to get a deep understanding of the relationship between GBs and degassing of residual hydrogen from HDDR–treated powders.

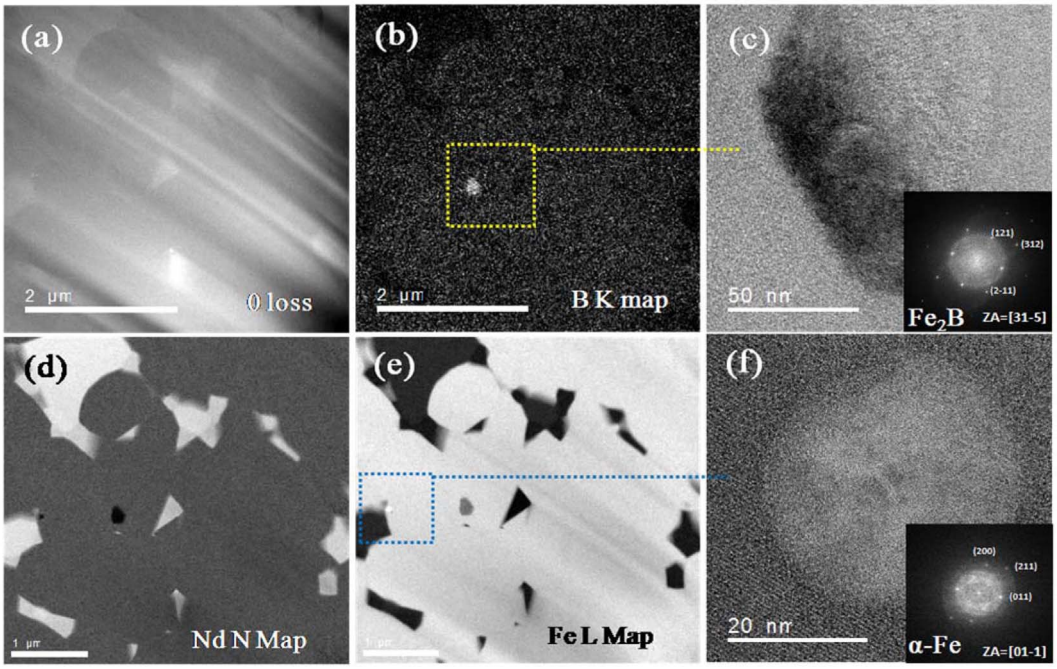

Fig. 3. (Color online) Energy filtered elemental mapping images and high–magnification bright field images of the HDDR–treated powder after GBDP with 6 wt.% Nd–Cu alloy at 800 °C using TEM.

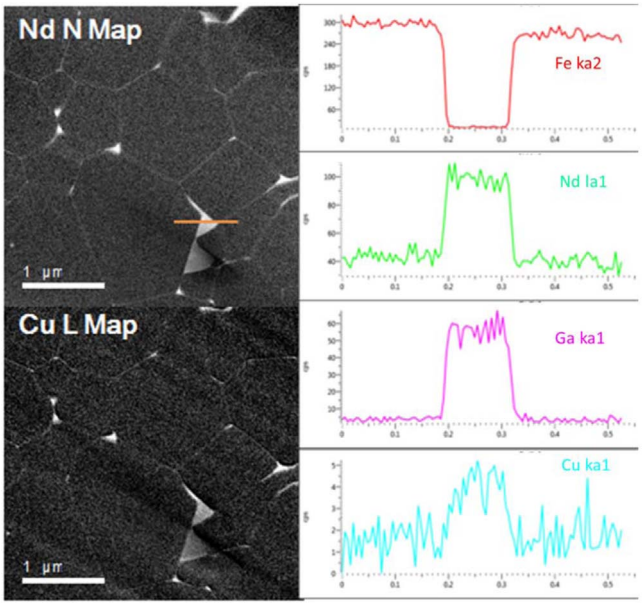

Fig. 4. (Color online) Elemental maps of Nd and Cu (left parts) and line scans (right parts) of the HDDR–treated powders after GBDP with 6 wt.% Nd–Cu alloy at 700 °C.

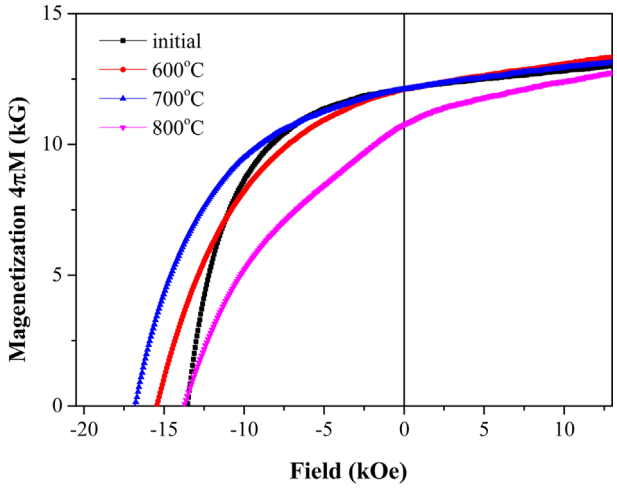

Fig. 5. (Color online) Demagnetization curves of the initial HDDR–treated powders and the HDDR–treated powders after GBDP with 6 wt.% Nd–Cu alloy at 600, 700 and 800 °C, respectively.

Figure 4 shows elemental maps and line scans obtained using TEM for the HDDR–treated powders after GBDP with 6 wt.% Nd–Cu alloy at 700 °C. The distinct bright contrast along the GBs suggests the continuous thin Nd–rich phase layers. The average concentration of Nd along GBs after GBDP was higher (16.0 at.%) than that (12.5 at.%) of initial HDDR–treated powders. This increased fraction could be resulted from the diffusion of molten Nd–Cu into the GBs. Furthermore, the concentration of Cu and Ga are higher along GB than that in the main phase. From the microstructural studies, it is clear that continuous thin Nd–rich phase layer around main phases lead to a better separation of them and the clear and

Table 1. Magnetic properties of the initial HDDR–treated powders and the HDDR–treated powders after GBDP with 6 wt.% Nd–Cu alloy at 600, 700 and 800 °C, respectively.

Samples	Coercivity (kOe)	Remanence (kG)	$(BH)_{max}$ (MGOe)
Initial HDDR	13.5	12.1	31.8
GBDP at 600 °C	15.4	12.1	32
GBDP at 700 °C	16.9	12.1	33
GBDP at 800 °C	13.7	10.8	14

smooth GBs. Moreover, the diffusion of Cu to the particles is beneficial to promote the wettability behavior and separation of main phase, leading to the homogeneous formation of Nd–rich phases, and results in high coercivity [22]. The microstructural modification after GBDP would be helpful to decrease the magnetic interactions among $Nd_2Fe_{14}B$ hard magnetic grains. Thus, any direct magnetic coupling of the $Nd_2Fe_{14}B$ grains could be reduced, which significantly improves the coercivity. The fine and uniform distribution of the $Nd_2Fe_{14}B$ grains and the modified GBs are important factors to improve the coercivity of Nd–Fe–B magnets.

Figure 5 shows the demagnetization curves of the HDDR–treated powders before and after GBDP with 6 wt.% Nd–Cu alloy at 600, 700 and 800 °C, respectively. The temperature for GBDP has a significant influence on the magnetic properties of HDDR–treated powders. The coercivity increases from 13.5 kOe for the initial HDDR–treated powders to 16.9 kOe for the powders after GBDP at 700 °C almost without remanence decrease (Table 1). The enhanced coercivity is attributed to the formation of the distinct GB phase which causes a weaker ferromagnetic interaction among the main grains. When the temperature of GBDP was further increased to 800 °C, the coercivity is almost same as that of the initial HDDR–treated powders while the remanence also decreased. This irregular dependence of the magnetic properties of the HDDR–treated powders on the GBDP temperature can be attributed to not only the grain growth and the distribution of Nd–rich phase through the GBs but also the residual hydrogen–related disproportionation during GBDP.

4. Conclusion

HDDR–treated Nd–Fe–B powders were modified by grain boundary diffusion process with Nd–Cu alloy. The temperature of GBDP with Nd–Cu has a significant impact on the microstructures of HDDR–treated Nd–Fe–B powders. The uniform distribution of Nd–rich both at the triple junction and along the GBs for the sample after GBDP at 700 °C gives rise to a remarkable increase of coercivity to 16.9 kOe compared with 13.5 kOe for the initial HDDR–treated powders. GBDP at 700 °C with Nd–Cu alloy is not only effect to isolate the main phases but also to prevent the residual hydrogen induced phenomenon. The residual hydrogen–related degassing and disproportionation process also worked during GBDP at 600 and 700 °C. When the temperature of GBDP was increased to 800 °C, the grown grains and disproportionation process lead to weaken magnetic properties [18, 23].

Acknowledgements

This research was supported by a grant from the Fundamental R&D Program for Core Technology of Materials funded by the Ministry of Knowledge Economy, Republic of Korea.

References

[1] J. F. Herbst, Rev. Mod. Phys. **63**, 819 (1991).
[2] S. Sugimoto, J. Phys. D: Appl. Phys. **44**, 064001 (2011).
[3] J. F. Herbst and W. B. Yelon. J. Appl. Phys. **57**, 2343 (1985).
[4] H. R. Cha, J. H. Yu, Y. K. Baek, H. W. Kwon, T. H. Kim, C. W. Yang, T. S. Lim, Y. D. Kim, and J. G. Lee, Met. Mater. Int. **20**, 909 (2014).
[5] H. R. Cha, J. H. Yu, Y. K. Baek, H. W. Kwon, Y. D. Kim, and J. G. Lee, J. Magn. **19**, 49 (2014).
[6] W. F. Li, T. Ohkubo, and K. Hono, Appl. Phys. Lett. **93**, 052505 (2008).
[7] R. Ramesh, G. Thomas, and B. M. Ma, J. Appl. Phys. **64**, 6416 (1988).
[8] K. Uestuener, M. Katter, and W. Rodewald, IEEE Trans. Magn. **42**, 2897 (2006).
[9] Y. Shinaba, T. J. Konno, K. Ishikawa, K. Hiraga, and M. Sagawa, J. Appl. Phys. **97**, 053504 (2005).
[10] J. D. Livingston, J. Appl. Phys. **57**, 4137 (1985).
[11] H. Sepehri-Amin, W. F. Li, T. Ohkubo, T. Nishiuchi, S. Hirosawa, and K. Hono, Acta Mater. **58**, 1309 (2010).
[12] J. Fidler, J. Magn. Magn. Mater. **80**, 48 (1989).
[13] H. Sepehri-Amin, T. Ohkubo, T. Nishiuchi, S. Hirosawa, and K. Hono, Scripta Mater. **63**, 1124 (2010).
[14] J. J. Ni, T. Y. Ma, and M. Yan, J. Magn. Magn. Mater. **323**, 2549 (2011).
[15] Z. Lin, J. Han, M. Xing, S. Liu, R. Wu, C. Wang, Y. Zhang, Y. Yang, and J. Yang, Appl. Phys. Lett. **100**, 052409 (2012).
[16] M. Takezawa, Y. Nagashima, Y. Kimura, Y. Morimoto, J. Yamasaki, N. Nozawa, T. Nishiuchi, and S. Hirosawa, J. Appl. Phys. **111**, 07A714 (2012).
[17] T. Nishiuchi, S. Hirosawa, M. Nakamura, M. Kakimoto, T. Kawabayashi, H. Araki, and Y. Shirai, IEEE Trans.

Elec. Elec. Eng. **3**, 390 (2008).
[18] M. A. Matin, H. W. Kwon, J. G. Lee, and J. H. Yu, IEEE Trans. Magn. **50**, 1 (2014).
[19] W. F. Li, T. Ohkubo, K. Hono, T. Nishiuch, and S. Hirosawa, Appl. Phys. Lett. **93**, 052505 (2008).
[20] H. Sepehri-Amin, D. Prabhu, M. Hayashi, T. Ohkubo, K. Hioki, A. Hattori, and K. Hono, Scripta Mater. **68**, 167 (2013).
[21] M. Matin, H. W. Kwon, J. G. Lee, and J. H. Yu, J. Magn. **19**, 106 (2014).
[22] S. Nishio, S. Sugimoto, R. Goto, M. Matsuura, and N. Tezuka, Mater. Trans. **50**, 723 (2009).
[23] B. D. Cullity and C. D. Graham, Introduction to Magnetic Materials. Addison-Wesley, London (1972) pp. 360-362.